Incorporating Satellite Imagery in Traffic Monitoring Programs

Mark R. McCord*
Carolyn J. Merry*
Prem Goel**

The Ohio State University
Center for Mapping
* Department of Civil & Environmental Engineering and Geodetic Science
2070 Neil Avenue
** Department of Statistics
1958 Neil Avenue
Columbus, Ohio 43210
USA
(614)292-2388 (voice)
(614)292-3780 (fax)
mccord.2@osu.edu

North American Travel Monitoring Exhibition and Conference
Charlotte, North Carolina USA
May 11-15, 1998

ABSTRACT

We report on investigations of the feasibility and usefulness of complementing traditional traffic count data with high resolution satellite imagery for traffic monitoring programs. Feasibility tests would be required to demonstrate that satellite data could be processed into accurate observations of traffic parameters. We anticipate comparing flow estimates obtained from automatic traffic recorders to estimates obtained from satellite images. To illustrate the comparisons and understand their limitations, we conducted two simulated field tests in the Central Ohio region. We converted measures made from aerial photographs into flow estimates for several facilities, compared these to concurrent estimates obtained from automatic traffic recorders, and found good agreement. We propose that unobservable changes in vehicle velocities will probably be the most limiting factor in getting good agreement when using real satellite data.

To be useful in monitoring programs, the satellite data would have to be processed and interpreted automatically. We discuss our strategy for identifying vehicles from satellite imagery. We illustrate the benefits of two components of this strategy, image subtraction and reflectance transformation, using scanned aerial photography to simulate panchromatic 1-m satellite imagery.

We develop a simulation and estimation program to investigate the improvement in estimates of vehicle miles traveled due to the incorporation of satellite imagery and report preliminary results of this investigation. We use the program to illustrate that the improvement in the estimates will depend to a large degree on the number of ground counts available.

1. Introduction

Anticipated availability of high resolution satellite imagery motivates a consideration of using satellites to collect traffic data. Previously, we estimated that approximately 1-m resolution panchromatic imagery should allow accurate vehicle counts and rough vehicle classifications, while large vehicles might be accurately detected with only 4-m resolution (McCord, et al., 1995b). At least three private groups are planning to market high resolution satellite data (American Society of Photogrammetry and Remote Sensing, 1996). EarthWatch lost the EarlyBird satellite (3-m panchromatic data) shortly after launch in December 1997. However, in 1999 they plan to launch the QuickBird-1 satellite with a 1-m panchromatic (0.5-0.9 µm) sensor and a 4-m multispectral (MS) sensor onboard. ORBIMAGE Spacecraft Control Center is presently developing OrbView-3, which will include a 1-m panchromatic and 4-m-multispectral sensor. In late 1998 Space Imaging EOSAT will launch Ikonos-1 with 1-m panchromatic and 4-m MS sensors.

Geostationary orbits, where the satellite remains stationary over a point on the equator, are convenient when rapid repetitive coverage is needed. However, to maintain a geostationary orbit, a satellite would need to orbit at altitudes of approximately 36,000 km, much too high to obtain the ground resolution required to detect vehicles (McCord, et al., 1995a). The image data obtained at lower earth orbits (400-1000 km) will consist of "snapshots" of different wide spatial areas taken at instants in time. Although the same area could be imaged on different orbits, the repeat periods would be on the order of days. We propose that such data would be most useful for complementing traffic monitoring programs such as those that collect and estimate state- or regionwide network traffic statistics. Compared to traditional ground-based methods, satellite imagery would detect concurrent traffic conditions on an increased number of highway segments. It could also more directly determine changes in conditions along a segment of highway. Figure 1-1 shows velocities along approximately 10 km of I-70 in Central Ohio estimated from overlapping aerial photography that we have been using to simulate satellite data (see, below, and Merry, et al., 1996).

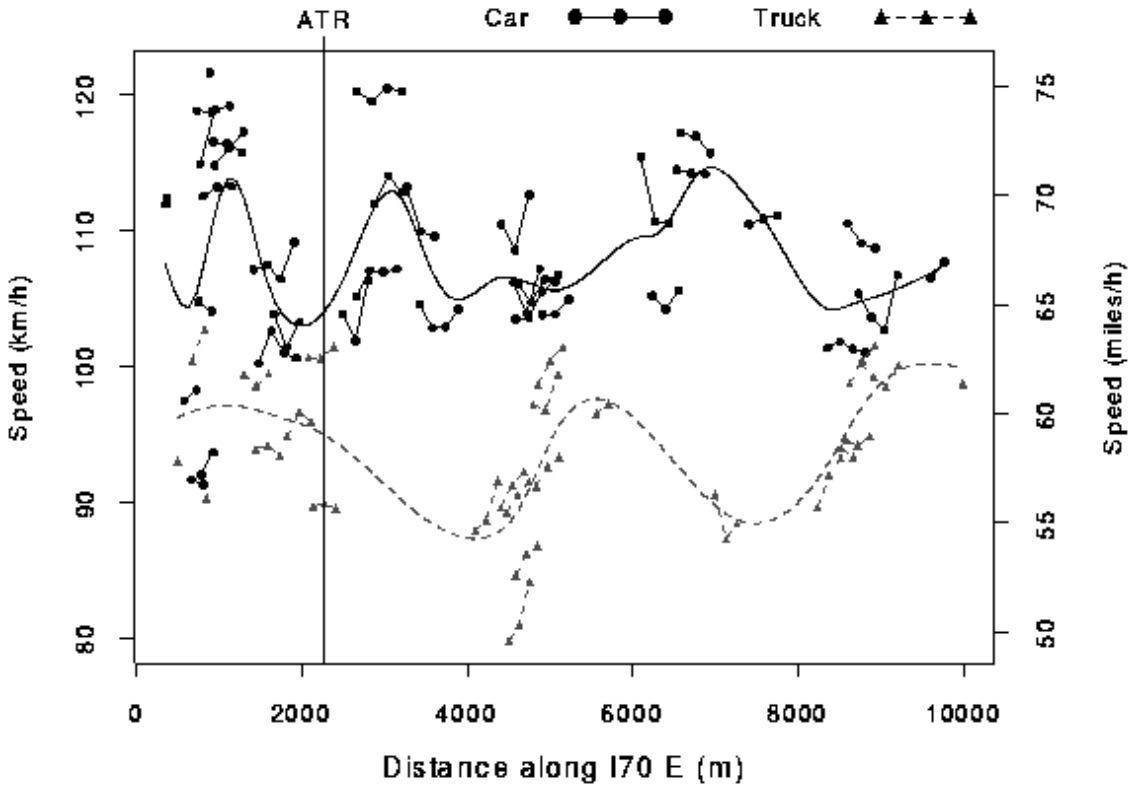

Figure 1-1 Velocity profile along I-70 Eastbound in Central Ohio, estimated from overlapping aerial photographs

Identifying vehicles in a single snapshot would provide direct vehicle density measurements at the time of the image. However, scheduled satellites will image the same location a few seconds apart, and we are presently investigating means to match identical vehicles imaged at different times. Vehicle speeds could then be determined by dividing the distances traveled by the time between the different images. In the absence of vehicle matching algorithms, an estimated average highway velocity could be substituted for individual vehicle speeds. Coupling highway velocities with imaged densities would generate estimates of traffic flow on the segment.

Several issues would have to be addressed, however, before satellite imagery could operationally be used to complement traffic monitoring programs. Among the issues, we see these needs: *i)* demonstrate that vehicles can be identified accurately from satellite imagery, *ii)* process the imagery efficiently into estimates of traffic characteristics, and *iii)* understand how and the extent to which the derived estimates can complement ground counts to improve network-wide estimates. We report on aspects of our investigation that address these needs in the following sections.

2. Air-ground coordinated field tests

We conducted two sets of field tests in which we determined flow rates from aerial photos and compared these rates with those concurrently obtained from automatic traffic recorders (ATR's). When available, using real satellite imagery in similar tests would be valuable in demonstrating the ability of estimating imagery-based traffic volumes on a large scale.

In our field tests, the Ohio Department of Transportation (ODOT) acquired aerial photographs with 60% overlap of Central Ohio interstate highway sections on 30 November 1995 and 29 October 1996. ODOT used volume-by-length ATR's to collect 1-minute volumes on the eastbound (EB) and westbound (WB) directions of I-70 in the 1995 and 1996 field tests, and on the northbound (NB) and southbound (SB) sections of I-71 in the 1996 field test. The volumes were classified into two length classes -- under 20 ft (6.1 m) and 20 ft (6.1 m) or over -- which we call "cars" and "trucks," for simplicity. ODOT used weigh-in-motion ATR's to record FHWA class and the time to the nearest second of vehicles passing the sensors on the northbound (NB) and southbound (SB) sections of I-270 in both 1995 and 1996. We considered FHWA classes 1, 2, 3, and 5 to correspond to our "car" category, and the other classes to correspond to our "truck" category. To provide additional control, we videotaped traffic at the sites during the data collection period.

From the photography we visually identified vehicles, their locations and those of the ATR's; designated each vehicle as either a "car" or "truck;" and assigned indicators to identify identical vehicles in different photographs. The 1995 information was entered directly on the photographs. Common locations were identified in overlapping images, and distances along the highway were measured from these common locations. The 1996 aerial photographs were scanned and saved as digital 8-bit image files. Vehicle

information (locations and identifiers) and highway edgelines were digitized from these image files, and vehicle locations were projected to the edgeline. Common control points were identified in subsequent images, and the images were resampled to a common coordinate system. From the vehicle identifiers, locations, and common reference systems, we determined linear highway distances traveled by vehicles during the time between the photographs. Distances were measured on the photographs with a ruler for the 1995 data and using standard image processing software with the digital 1996 data. Dividing by the time between the photographs, we estimated the vehicle velocities. Knowing the locations of the ATR's and the vehicles to a common reference system, the times the vehicles were photographed, and the vehicle velocities, we estimated the times that the vehicles would pass the ATR's. Cars were assumed to travel at a constant velocity equal to the average velocities of identified cars in a specified length of the highway. Similarly, trucks were assumed to travel at an average truck velocity in this length of highway. The length for computing average speed was determined by a first approximation of the section of highway containing vehicles that would pass the ATR during the time interval of interest.

The estimated times at which the vehicles would pass the ATR's discussed above would correspond to the aircraft clock. However, the ATR, video, and aircraft clocks were not exactly synchronized to each other. We compensated for time discrepancies by adding or subtracting a constant time offset between clocks (Merry, et al., 1996). The time offsets between the ATR and video clocks were determined to maximize Pearson's correlation coefficient between counts taken from the two data sources. The time offsets between the photo and video clocks were determined by estimating the times that specific vehicles in both the air photos and videos passed the ATR's on the respective clocks, and averaging the differences in these times. The time offsets between the photo and ATR clocks were determined by taking the differences of these photo-video and ATR-video time offsets.

After compensating for the time discrepancies among the various clocks, we compared volumes-by-class passing the ATR's estimated from the images, estimated by video, and recorded directly by the ATR for an estimated concurrent time interval. We considered the longest time intervals such that vehicles using entrance and exit ramps would not confound the comparisons. That is, we determined the time intervals by estimating the earliest and latest times that imaged vehicles downstream of upstream ramps and upstream of downstream entrance ramps would pass the ATR's, where upstream and downstream directions are defined with respect to the ATR. We shortened the interval to the nearest minute for the volume-by-length ATR's and to the nearest second for the WIM-based ATR's.

The estimated volumes are presented in Table 2-1. In general, the estimates compare favorably at the I-70 and I-71 sites and less favorably at the I-270 site. We were unable to obtain concurrent video at the I-270 site in the 1995 test, but the video data in the 1996 test support the quality of the photo-based estimates. Upon detailed investigation, we found that the (WIM) ATR was malfunctioning during the 1996

comparison interval. We did not investigate the I-270 ATR as closely in the 1995 test, but we have confidence that our procedure, and especially our semi-automated procedure used on the 1996 data, can produce good estimates of volumes past an ATR location.

		CAR VOLUME			TRUCK VOLUME	
Segment	ATR	Photo	Video	ATR	Photo	Video
I-70 WB,1995 Time Interval = 2 minutes	12	13	13	11	11	10
I-70 EB,1995 Time Interval = 1 minute	10	10	10	9	9	9
I-270 NB, 1995 Time Interval = 2 minutes	46	39	na	14	14	na
I-270 SB, 1995 Time Interval = 3 minutes	42	64	na	61	28	na
I-70 WB,1996 Time Interval = 6 minutes	63	72	64	47	42	45
I-70 EB,1996 Time Interval = 2 minutes	16	16	16	11	12	12
I-270 NB, 1996 Time Interval = 0.83 minute	18	31	28	13	6	6
I-270 SB, 1996 Time Interval = 1.58 minutes	52	45	47	3	10	10
I-71 NB, 1996 Time Interval = 2 minutes	25	27	26	7	7	5
I-71 SB, 1996 Time Interval = 6 minutes	52	53	na	32	30	na

Table 2-1 Volumes passing ATR estimated from air photos and videos and recorded by ATR's during estimated concurrent time intervals

We have confidence in our procedure that processes digitized information on vehicle locations and identifiers to estimate volumes past an ATR location during a specified time interval. We are presently investigating the contributions of various sources of error in these estimations. Errors due to pixel resolution, digitization of vehicle locations, and projected locations along digitized highway edgelines seem minor. It appears that errors due to estimating time offsets and resampling of images could be more important. However, in a test using real satellite data, the time offset errors could be reduced by ensuring that the ATR clock is calibrated against a GPS clock, which would be the time of the satellite image. The error due to resampling overlapping images should also be reduced because of the precise locations associated with the satellite images. The most important and, perhaps, most irreducible source of error in estimating when vehicles imaged at a given time would pass an ATR appears to be the error in determining the velocity profile of the vehicle between the time that the vehicle was

imaged and when it passed the ATR. We are presently trying to develop a means to get some sense of the likely magnitude of this error, but we are encouraged by the performance of the empirical results in Table 2-1.

3. Image processing

If satellite imagery were to be used in traffic monitoring programs on an operational basis, the imagery would have to be processed into the needed information with a high degree of automation. We have been investigating various image processing approaches using scanned aerial photography to simulate satellite imagery. The photographs are scanned to produce 8-bit digital images corresponding to 1-m resolution (Merry, et al., 1996; McCord, et al., 1995a). The approach that we believe to be most promising for automatic vehicle detection and identification is one that would identify individual pixels as being dynamic or static--i.e., those whose reflectance values are believed to have changed with time and those whose reflectance value are not believed to have changed with time--and then to consider the spatial correlation of dynamic pixels with other neighboring dynamic pixels to estimate vehicle locations and classifications.

Because the dynamic pixels are associated with movement, they would primarily correspond to moving vehicles on the highway. However, the dynamic pixels could also correspond, for example to sign shadows, which change with the sun angle, and cloud shadows which appear with less predictability. The spatial relations among neighboring pixels, along with information about static physical structures (e.g., signs) that cast shadows on the highway would help refine vehicle counts and classification estimates. We envision that the basic information in our procedure would consist of a weight or belief value that each value is dynamic. Here, we report on our investigations into the use of image subtraction and transformation, which we believe will be two important processes in developing this characterization of the pixel as being either dynamic or static.

Subtracting the reflectance values in a satellite image taken at time *t* from the estimated reflectance values of an image representing the static background (i.e., the pavement) of the highway should highlight the dynamic pixels. Subtracting reflectance values of a pixel in the time *t*-image corresponding to pavement from the reflectance values of the pixel at the same location in the background image representing pavement would leave a value of zero, if the pavement reflectance in the background image was the same as that of the pavement at the same location in the time *t*-image. However, the difference would probably not be exactly zero because of a systematic change in lighting conditions, random noise in reflectance measurements, and an inability to match pixel locations exactly. We attempt to correct for the first effect, the systematic change in lighting conditions, by transforming the reflectance values in the background image to match the reflectance values corresponding to pavement in the time *t*-image, which we discuss below. Random noise and inability to match pixel location exactly between the time *t*-image and the background image will keep reflectance differences of static pixels

from being exactly zero, but we expect that the magnitudes of these difference would be much less than those of the differences between the reflectance values of pixels corresponding to dynamic objects (mostly vehicles) in the time *t*-image and the reflectance values of pixels at the same location in the background image representing pavement.

The repeat orbits of the satellites would mean that many images of the same location would be available. The static background image could be obtained on low density highways by averaging the reflectance values of the images. The low density would mean that the dynamic signals would have a low probability of occurring at exactly identical locations in pairs of images, and the static signals would dominate in the average. Higher density highways would require a more sophisticated procedure.

As mentioned above, different lighting conditions may imply that a pixel corresponding to pavement may have a different reflectance value than the same pixel corresponding to the same pavement on a different day. Therefore, we propose first transforming the reflectance values in the static background image to match the reflectance values of pixels estimated to be pavement in the time *t*-image. Doing this assumes that static and dynamic pixels can be distinguished in the time *t*-image, which is the original goal. Therefore, we are working on an iterative procedure, where the subtraction is performed at each iteration, and pixels with differences far from zero receive greater weights or degrees of belief corresponding to dynamic pixels.

To illustrate the effect of the subtraction and the transformation, consider the scanned and simulated background images in Figure 3-1. The scanned image represents the time *t*-image. We formed the background image by manipulating an image of the same location taken approximately 5 seconds earlier. Specifically, we visually determined which pixels in this background image corresponded to vehicles, replaced the reflectance values of these vehicle pixels by reflectance values of neighboring pixels in the image that were visually determined to correspond to pavement; and changed the brightness level. In Figure 3-2, we plot the reflectance values of pixels in the time *t*-image against those of the corresponding pixels in the simulated background image. We fit a smoothing-spline function through those points corresponding to the pavement pixels. The resulting fit is nonlinear in this case, indicating the need to consider nonlinear transformations between the time *t*-image and the background image.

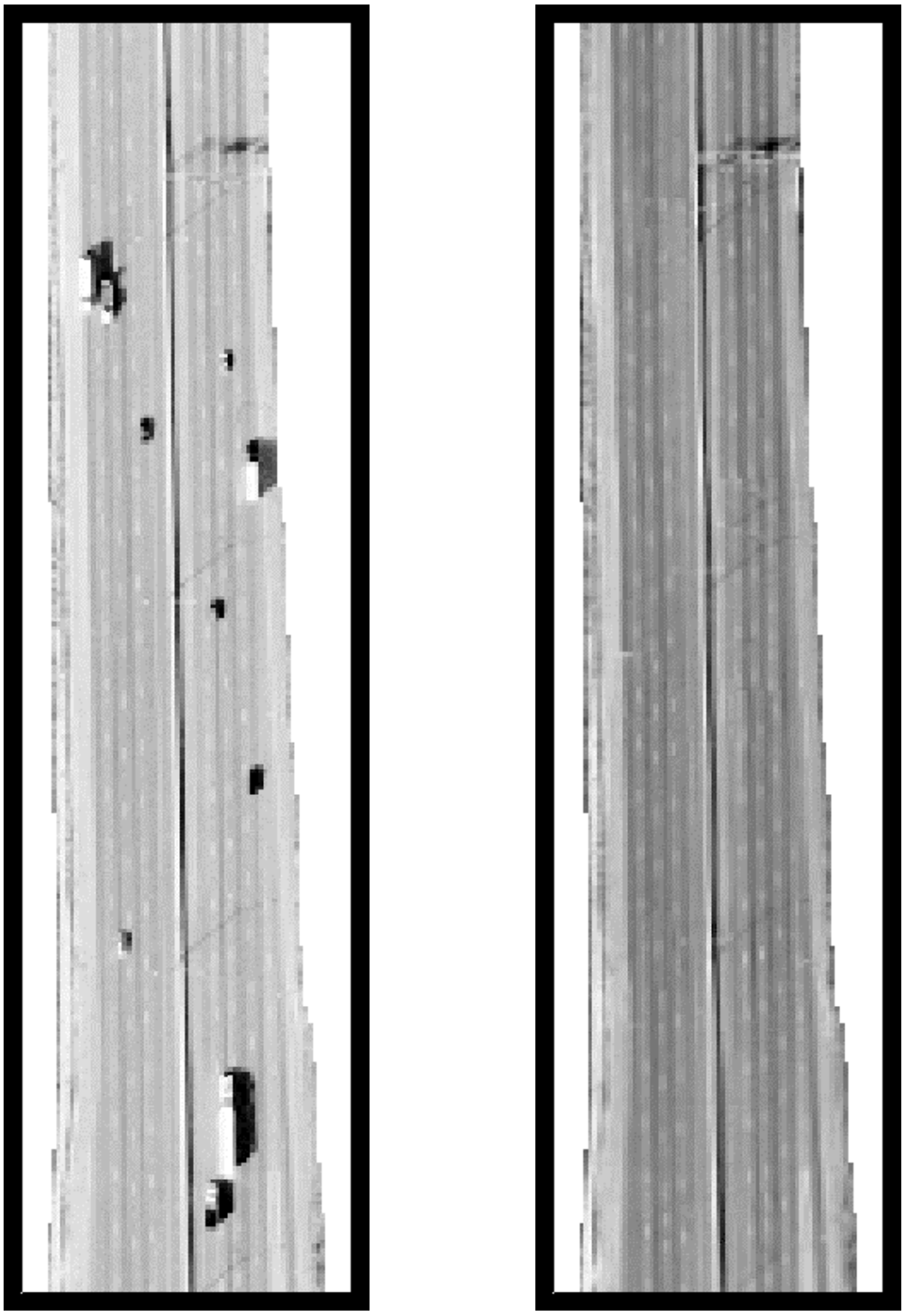

Figure 3-1 Scanned image representing time *t*-image and simulated background image

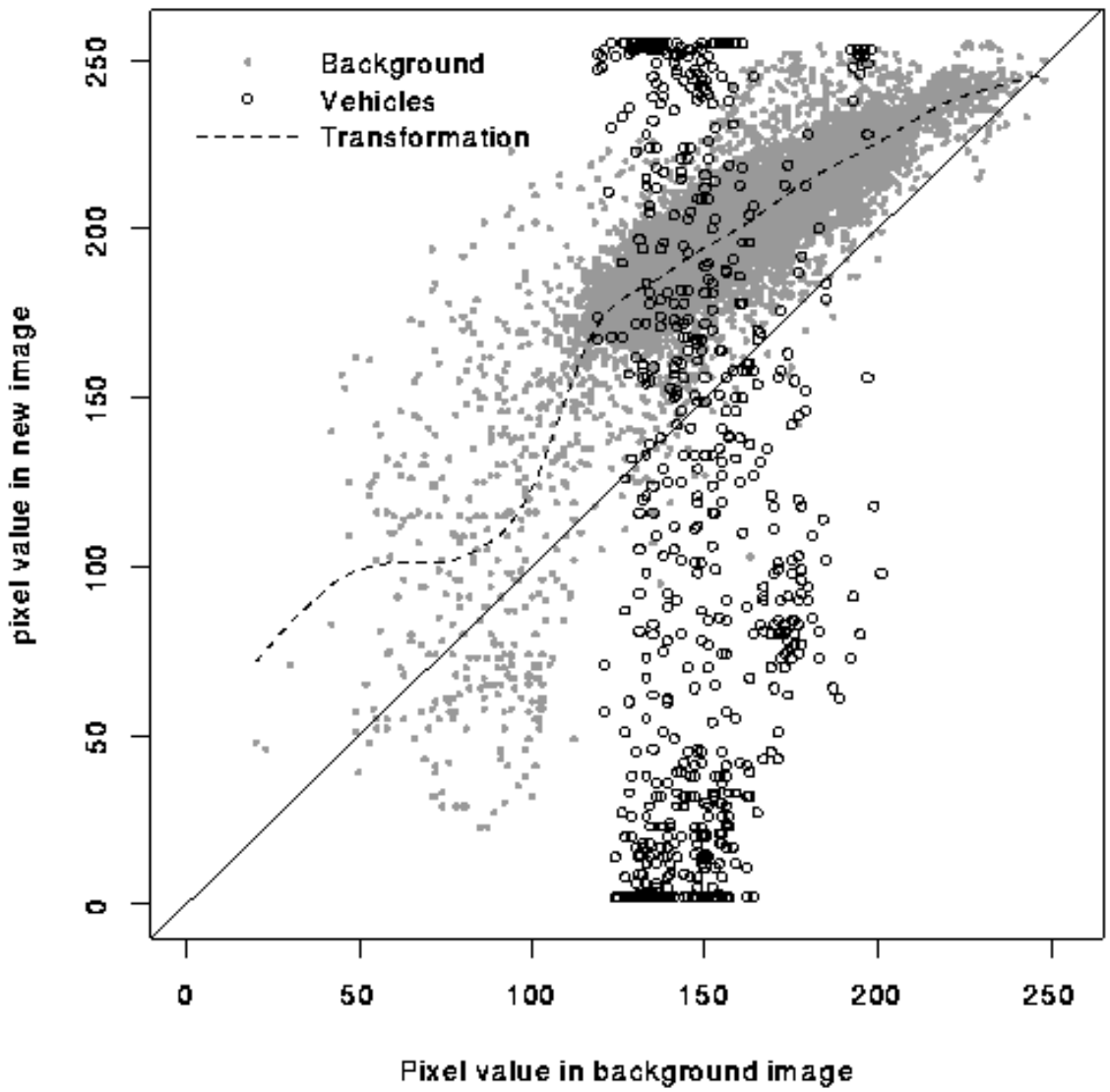

Figure 3-2 Reflectance values of pixels in time *t*-image vs. reflectance values in simulated background image (dashed curve represents smoothing-spline transformation)

Based on a visual classification, there are 662 pixels corresponding to vehicles in the time *t*-image. We use this information to consider three methods of distinguishing between vehicle and pavement pixels. The first method represents a "thresholding" method (McCord, et al., 1995a,b) without image subtraction. In this method, we "label" as vehicle pixels the 331 pixels in each tail of the reflectance value histogram; we call the other pixels pavement pixels. The second method subtracts the time *t*-image from the background image without transforming the background. In this method, we label as vehicle pixels the 662 pixels with the largest absolute differences in reflectance values; we call the other pixels pavement pixels. The third method is intended to investigate the

added advantage of transforming the background before subtracting. In this method, we transform the reflectance values in the background image according to the smoothing-spline function shown in Figure 3-2, subtract the time *t*-image from this transformed image, and label as vehicle pixels the 662 pixels with the largest absolute differences in reflectance values; we call the other pixels pavement pixels. We present the results in Table 3-1. We see that the "subtraction without transformation" method markedly increases the percentage of correctly classified vehicle pixels compared to the thresholding method, and that transforming before subtraction again markedly increases the percentage of correctly classified vehicle pixels.

METHOD	% CORRECTLY CLASSIFIED VEHICLE PIXELS (OUT OF 662)
No Subtraction ("Thresholding")	54
Subtraction Without Transformation	65
Subtraction With Transformation	74

Table 3-1 Empirical performance of three methods in identifying vehicle pixels

4. Contribution of satellite data to VMT estimates

As mentioned above, the satellite data would consist of "snapshots" of the highway segments at instants in time. Several snapshots could be obtained over time, and the greatest benefit in the satellite data might be found in identifying spatial patterns in traffic characteristics. For example, the data might indicate consistently high or low velocities on certain segments. These indications could then be confirmed with traditional spot speed studies. Or, the series of snapshots might show that certain segments exhibit temporal patterns different from those of other segments in the same traffic monitoring sampling class. Aggregate estimates could then be improved by redefining the sampling classes.

Despite this potential for observing abnormal or unexpected traffic patterns, we limit our analysis here to the potential of satellite data to improve traffic estimates by increasing the number of observations of highways segments, even though the additional observations cover only a limited time period. We conduct our analysis using Monte Carlo simulation, and consider the estimation of annual vehicle miles traveled (VMT) for a group of *N* segments in a single "highway class." We consider segments to be in the same highway class if they have the same underlying daily and monthly expansion factors. We generate satellite and traditional ground observations from a deterministic model reflecting systematic components of temporal traffic patterns and stochastic components reflecting random variations to these systematic components. We then compare estimated VMT in two ways: *i)* with the simulated traditional ground observations only; and *ii)* with the traditional ground observations combined with the

simulated satellite observations. We assume that the observations are error-free, and, therefore, that any errors in the VMT estimates stem from the incomplete sampling of the segments through time.

Our analytical system consists of a simulation and estimation component. In the simulation component, we input a number of segments N for the class. We randomly generate lengths l_s and average annual daily traffic $AADT_s$, $s = 1, 2, ..., N$, and calculate the true VMT for the simulation run as:

$$\text{VMT} = \sum_{s=1,...,N} l_s \, AADT_s. \qquad (3\text{-}1)$$

To simulate volumes obtained from ground counts, we specify a number C of continuous (permanent) automatic traffic recorders (ATR's) and a number P of two consecutive 24-hour counts that can be obtained from the portable ATR's in the year. We then simulate true 24-hour volumes on C of the segments for 365 sequential days. To simulate observations from portable counters, we also randomly generate P segment-day pairs and two consecutive 24-hour volumes for the segment in the segment-day pair beginning on the day of the pair. We assume that we collect these true volumes without error. To simulate an error-free 24-hour volume $VOL^{(g)}_{s,t}$ collected from a traditional ground count for any day (time) t, $t \in \{1, 2, ..., 365\}$, on segment s, $s \in \{1, 2, ..., N\}$, we:

i) determine the month $m(t) \in \{1, 2, ...,12\}$ and day-of-week $d(t) \in \{1, 2, ..., 7\}$, corresponding to day-of-the-year t;
ii) use exogenously specified month-of-year and day-of-week expansion factors $F^{(m)}_{m(t)}$ and $F^{(d)}_{d(t)}$, respectively, and the segment $AADT_s$ generated above;
iii) generate a random error term $\varepsilon_{m,d}$ from a normal distribution with mean 0 and variance $\sigma^2_{m,d}$ and compute:

$$\text{VOL}^{(g)}_{s,t} = \text{AADT}_s \, [\text{F}^{(m)}_{m(t)}{}^{-1}] \, [\, \text{F}^{(d)}_{d(t)}{}^{-1}] \exp(\varepsilon_{m,d}), \, . \qquad (3\text{-}2)$$

where *exp(.)* is the inverse function of the natural logarithm. In (3-2) a systematic component of temporal variation--namely, $AADT_s \, F^{(m)}_{m(t)}{}^{-1} \, F^{(d)}_{d(t)}{}^{-1}$--is multiplied by a random component $exp(\varepsilon_{m,d})$ to determine the actual volume. We specify the expansion factors $F^{(m)}$ and $F^{(d)}$ so that they would represent expansion of the average volumes on a given month or day to the AADT--i.e., $(1/12)\sum_{\forall m} F^{(m)}_{m}{}^{-1} = (1/7) \sum_{\forall d} F^{(d)}_{d}{}^{-1} = 1$--and use $exp(\varepsilon_{m,d})$ as the random component to ensure positive volumes, while maintaining distributional assumptions. We also generate random error terms so that 365 days of generation will yield an average 24-hour volume equal to the AADT.

The density and velocity observations obtained from satellite data can be converted to flow rates past a fixed location during a short interval (see Section 2). These flow rates could be expanded to 24-hour volumes. Hourly and sub-hourly fluctuations would limit the accuracy in estimating 24-hour volumes from these flow rates. We

account for this additional randomness by generating a random error term $\varepsilon^{(sat)}_{m,d}$ from a normal distribution with mean 0 and variance $\sigma^{(sat)2}_{m,d}$ larger than that used in the distribution leading to the random term for volumes observed from ground counts. We input a satellite repeat period and coverage percentage *CVG* that indicates the proportion of segments that can be seen in a snapshot during one repeat pass of the satellite. We then randomly generate *N*CVG* segments that can be imaged by the satellite on each repeat pass. For each of these *N*CVG* segments, we generate 24-hour volumes $VOL^{(sat)}_{s,t}$ corresponding to the day of the year *t* on which the satellite is calculated to pass. We generate $VOL^{(sat)}_{s,t}$ in the manner described above, except that we use $\varepsilon^{(sat)}_{m,d}$ instead of $\varepsilon_{m,d}$ in (3-2).

In the estimation component, we estimate vehicle miles traveled $VMT^{w/o}$ in the case where satellite data would not be available (i.e., the "without" satellite scenario) and VMT^{w} in the case where it would be available (i.e., the "with" satellite scenario). To estimate $VMT^{w/o}$, we estimate AADT's for each segment based on the ground counts. We assume that the segments have been ordered such that the *C* segments with continuous ATR's are numbered first, the *NP* segments for which at least one portable count has been taken in the year are numbered next, and the *N-(C+NP)* segments for which no counts are taken are numbered last.

We calculate AADT's for the *C* segments with continuous ATR's as:

$$AADT^{(g)}_s = \sum_{s=1,...,365} VOL^{(g)}_{s,t} / 365, \qquad s = 1, 2, ...C; \qquad (3\text{-}3)$$

and estimate month-of-year and day-of-week expansion factors $F'^{(m)}$ and $F'^{(d)}$ factors from the daily volumes obtained from the *C* continuous ATR's as:

$$F'^{(m)} = [AADT^{(g)}_s / < VOL^{(g)}_{s,t} >_{m(t)=m}]_{s \in \{1,...C\}}, \qquad m = 1, 2, ..., 12; \qquad (3\text{-}4)$$

$$F'^{(d)} = [AADT^{(g)}_s / < VOL^{(g)}_{s,t} >_{d(t)=d}]_{s \in \{1,...C\}}, \qquad d = 1, 2, ..., 7; \qquad (3\text{-}5)$$

where $[\,.\,]_{s \in \{1,...C\}}$ represents the harmonic average over the *C* segments with continuous ATR's, and $< . >_{m(t)=m}$ and $< . >_{d(t)=d}$, respectively, represent arithmetic averages over all days-of-year *t* in month *m* and all days-of-year *t* that are day-of-the-week *d*. We estimate AADT's for the segments where counts have been taken with portable ATR's as:

$$AADT^{(g)}_s = < VOL^{(g)}_{s,t} F'^{(m)}_{m(t)} F'^{(d)}_{d(t)} >, \qquad s = C+1, ..., C+NP; \qquad (3\text{-}6)$$

where $< . >$ again represents the arithmetic average, and the average is taken over all days *t* on which portable counts on segment *s* have been taken. We estimate AADT's for segments with no count data in the year as the average of the AADT's estimated in (3-5) and (3-6):

$$AADT^{(g)}_s = (\sum_{s'=1,..,C+NP} AADT^{(g)}_{s'}) / (C+NP); \qquad s = C+NP+1, ..., N. \qquad (3\text{-}7)$$

Finally, we calculate:

$$VMT^{w/o} = \sum_{s=1,...,N} l_s \, AADT^{(g)}_s. \quad (3\text{-}8)$$

To estimate vehicle miles traveled VMT^w in the case where satellite data would be available, we first estimate $AADT^w_s$, $s = 1, 2, ..., N$, the AADT on each segment using both ground and satellite information, and calculate:

$$VMT^w = \sum_{s=1,...,N} l_s \, AADT^w_s. \quad (3\text{-}9)$$

We use (3-3) and ground counts only to estimate $AADT^w$ for the C segments with continuous ATR's. For all segments where at least one observation has been obtained from either portable ATR or satellite, we treat the estimated 24-hour volumes estimated from satellites like 24-hour volumes obtained directly from portable ATR's and use (3-6), averaging all observations with equal weight, regardless of whether the observation was obtained from an ATR or a satellite. We use the same expansion factors used when estimating AADT from ground counts only, i.e., the factors calculated using (3-4) and (3-5) with data from the continuous ATR's. We again estimate the AADT for the segments where no observations were obtained either from ground count or satellite as the average of the AADT's of the segments for which at least one observation was obtained, and weight all the AADT's in the average equally, regardless of whether they came from continuous ATR's, portable ATR's without satellite observations, portable ATR's with satellite observations, or satellite observations without ATR's. We are investigating more appealing ways of incorporating satellite estimates, but we use this *ad hoc* method here as a first-cut approach.

To investigate the contribution of adding satellite data to traditional ground counts, for each simulation run we form the percentage differences from the true VMT $PCD^{w/o} = (VMT^{w/o} - VMT)/VMT$ and $PCD^w = (VMT^w - VMT)/VMT$ of the estimates without and with satellite data and take the ratio of the absolute values of the PCD's:

$$Rpcd = |PCD^w| / |PDC^{w/o}| = \quad |VMT^w - VMT| / |VMT^{w/o} - VMT|. \quad (3\text{-}10)$$

Note that a value of *Rpcd* greater than unity indicates that the percentage error with the satellite data is greater than that without the data, and vice-versa. The ratio could be greater than unity, since estimating volumes from the snapshots could lead to very bad estimates of AADT's, and one might be better off ignoring the data.

To illustrate the program, we considered two scenarios. Both scenarios contained a single class of highways, with $N = 100$; $C = 1$; $\sigma^{(sat)2}_{m,d} = 2\sigma^2_{m,d} = 0.4$, $\forall m,d$; $AADT \sim Uniform[10{,}000; 90{,}000]$; and a typical set of monthly and daily expansion factors (McShane and Roess, 1990). We assume that the satellite images 100% (i.e., *CVG* =

1.0) of the segments once every 35.17 days. In the first scenario, we simulate 30 portable 24-hour counts per year; in the second scenario we simulate 5 portable 24-hour counts per year.

We plot the distributions of the *Rpcd* values for the two scenarios in Figure 4.1. The results give us confidence that the simulation and estimation programs are working as expected. hen there are enough ground counts available (represented here by the increased number of portable counts in Figure 4-1 a) the short term estimates provided by the satellite data used in the *ad hoc* manner considered so far will worsen aggregate estimates. On the other hand, when the number of ground counts is low, even the crude manner in which the ground and photo data are combined could improve the accuracy of the aggregate estimates. Although we tried to use realistic input parameters in the two scenarios, we need more work before we can use the simulation results for more than illustrative purposes. Once we have more faith in the magnitudes of the relative errors produced we could use this program to investigate trade-offs between the number of portable counts and satellite coverage, for example. We are also investigating more statistically-based ways to use the satellite data to improve estimates.

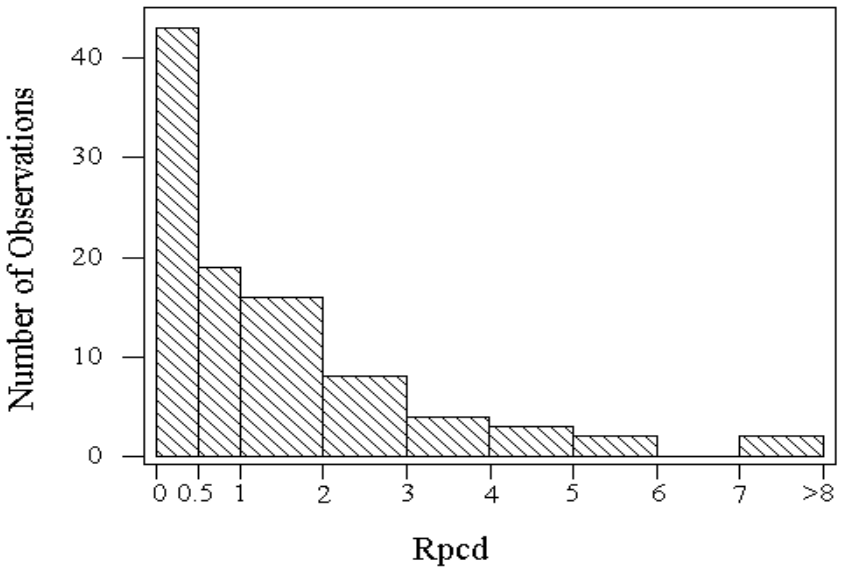

4-1a

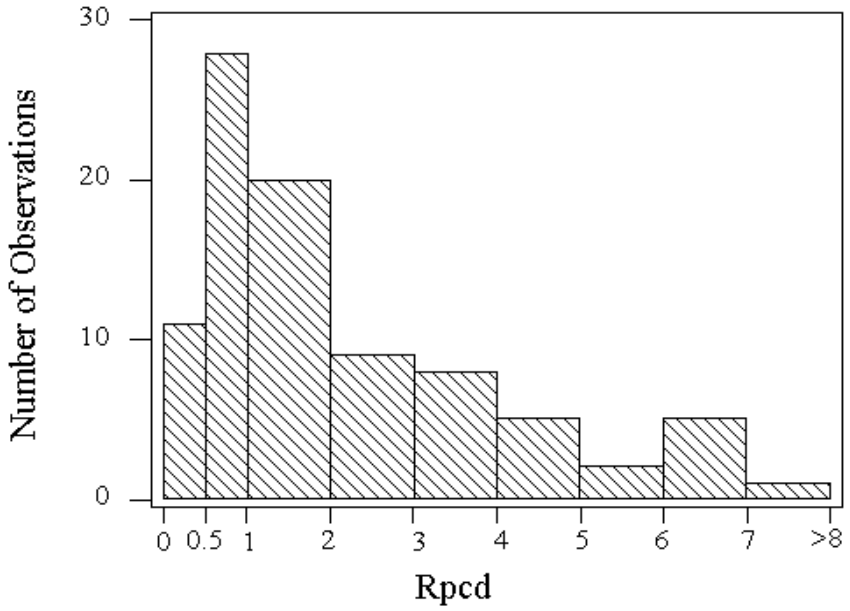

4-1b

Figure 4-1 Histograms of *Rpcd* in two scenarios
4-1a Relatively high number of portable ground counts available
4-1b Relatively low number of portable ground counts available

5. Conclusions

Our long-term objective is to test the feasibility of counting and classifying vehicles from high resolution satellite imagery and, if feasible, to determine how to exploit the imagery to improve the efficiency of traffic monitoring programs. We have been conducting tests and developing concepts using aerial photographs scanned at rates to simulate 1-m satellite imagery. We look forward to verifying our encouraging results and testing concepts developed with soon-to-be-available satellite imagery.

The results obtained in our air-ground coordinated field tests lead us to believe that we are now in a position to compare satellite image-based estimates of volumes passing an automatic traffic recorder (ATR) with recorded volumes while controlling for some factors that could skew the comparisons and understanding the relative impacts of others. Moreover, once the edgelines and vehicle locations and identities are digitized from the satellite images, the comparisons can be performed efficiently with software we

have developed. The good agreement we witnessed between photo-based volume estimates and ATR recordings also illustrates that, once digitized, the image information can be converted efficiently into accurate estimates of vehicle volumes during short time periods. Vehicle density is a more direct measure obtained from the image, and we do indeed obtain this measure, as well (see Merry, et al. 1996). Still, current practice is to collect and manipulate volume measurements, and we feel that traffic monitoring programs would more readily use satellite-based volume estimates than satellite-based density observations.

In the near future, we envision conducting similar tests using satellite imagery by visually identifying vehicles from images and encoding the information in digital files much like we did in the field tests reported here. However, if the imagery is to be used operationally in traffic monitoring programs, the vehicle information will have to be obtained in a more automated fashion. We are presently developing a procedure that: *i)* transforms the background image to the environmental conditions of the new image; ii) associates a weight to each pixel reflecting a degree of confidence that the pixel is dynamic; iii) classifies clusters of pixels based on relationships of the dynamic pixels with other neighboring dynamic pixels. We are encouraged by the results obtained for steps *i)* and *ii)* when using subtraction and transformation techniques. We plan to repeat this analysis for several images. In the test reported here, we visually determined the pixels upon which to base the transformation and implicitly assigned pixels weights of either 1 or 0 to label a pixel as dynamic or not. In practice, steps *i)* and *ii)* would have to be iterated to make this determination, and we are developing a process that updates continuous weights between 0 and 1 to converge on a final determination of dynamic pixels. We hope to report results soon on this process and the cluster classification procedure in step *iii).*

We recently developed the simulation and estimation program reported here. We expect it to be a powerful tool that we shall use to analyze the effectiveness of using the satellite data in alternate ways. We look forward to refining parameter estimates that are used as inputs to the program and broadening its scope to investigate the impact of using the satellite data in additional ways, such as redefining sampling classes.

ACKNOWLEDGMENTS

This work was supported by the Federal Highway Administration, through the Ohio Department of Transportation, under agreement no. 8494 to The Ohio State University, Center for Mapping. We gratefully acknowledge the assistance of Roger Bilisoly, Prof. John Bossler, Fatmeh Jafar, Gardar Johannesson, H. Carolyn Kan, and Hisanori Tomitaka.

REFERENCES

American Society of Photogrammetry and Remote Sensing, 1996. Land satellite information in the next decade "The World Under a Microscope," Executive Summary, American Society of Photogrammetry and Remote Sensing, Bethesda, Maryland, 72 p.

McCord, M.R., C.J. Merry, and J.D. Bossler, 1995a. The feasibility of traffic data collection using satellite imagery, Final Report to Federal Highway Administration, The Ohio State University, Research Foundation, Columbus, Ohio, April, 208 p.

McCord, M.R., C.J. Merry, X.D. Sun, and F. Jafar, 1995b. Resolution Effects on Vehicle Counts and Classification through Remote Sensing, *Journal of the Transportation Research Forum,* 35(1), pp. 41-52.

McShane, W.R., and R.P. Roess, 1990. *Traffic Engineering.* Prentice-Hall, Englewood Cliffs, NJ, 660 p.

Merry, C.J., M.R. McCord, J.D. Bossler, F. Jafar, and L.A. Perez, 1996. The feasibility of using simulated satellite data coordinated with traffic ground counts, Final Report to The Ohio Department of Transportation, The Ohio State University, Research Foundation, Columbus, Ohio, August, 77 p.